DISCUSSION PAPER Nº IDB-DP-1108

The Impacts of Air Quality Critical Episodes:

Evidence from Santiago (Discussion Paper)

Patricio Dominguez
Bridget Hoffmann
María Paula Medina-Pulido

Inter-American Development Bank
Department of Research and Chief Economist
November 2025

The Impacts of Air Quality Critical Episodes:

Evidence from Santiago (Discussion Paper)

Patricio Dominguez*
Bridget Hoffmann**
María Paula Medina-Pulido***

* Pontificia Universidad Católica
** Inter-American Development Bank
*** University of California, Davis

Inter-American Development Bank
Department of Research and Chief Economist

November 2025

Abstract

We document that lower-income individuals in Santiago, Chile are exposed to higher concentrations of PM10 and PM2.5 while at home and when taking into account their locations throughout the entire day. The exposure gradient across income deciles when assuming individuals are at their residence 24 hours a day is similar to that when considering their location at each hour of the day as reported on the reference day in an origin-destination survey. We use a fuzzy regression discontinuity design to explore the effect of the declaration of critical air quality episodes, which activate city-wide restrictions on private vehicles among others, on air pollution concentrations. We find that the declaration of critical air quality episodes leads to small and mostly statistically insignificant decreases in air pollution overall but the effects vary considerably across monitoring stations and hours of the day.[1]

JEL classifications: Q53; D30

Keywords: Air pollution; Air quality episodes; Command-and-control policy; Chile

[1]**Acknowledgements:** Corresponding author: Bridget Hoffmann (bridgeth@iadb.org), 1300 New York Ave., NW, Washington, DC.. The authors gratefully acknowledge funding from the Clean Air Fund through IDB TC RG-T4014. Marcos Paulo Rodrigues Correia, Karla Hernandez, and Estefania Vera Laborde provided excellent research assistance. Opinions, findings, conclusions, and recommendations expressed here are those of the authors and do not necessarily reflect the views of the Inter-American Development Bank.

1 Introduction

Air pollution has causal impacts on physical and mental health, labor supply and productivity, migration, cognitive performance, human capital accumulation, and decision-making (Hoffmann and Rud, 2024; Aguilar-Gomez et al., 2022; Chen et al., 2024, 2022; Guidetti et al., 2021; Anderson, 2020; Kahn and Li, 2020; Zivin et al., 2020; Chang et al., 2019; Deryugina et al., 2019; Zhang et al., 2017; Arceo et al., 2016; Graff Zivin and Neidell, 2013).

Policymakers in many cities around the world rely on command-and-control policies that activate temporary restrictions, including restrictions on driving, to reduce spikes in air pollution. However, these policies have different impacts on air quality in different neighborhoods of the city and may have different consequences for air pollution exposure across the income distribution.

In this paper, we explore the impacts of a command-and-control policy to reduce spikes in air pollution in Santiago, Chile. Santiago, Chile experiences high concentrations of particulate matter and the government can declare critical air quality episodes when particulate matter spikes. These episodes activate 24 hour restrictions including limits on road usage for public transportation, private vehicle restrictions, bans on agricultural burning, bans on the operation of cargo vehicles, and limitations on heating system usage.

First, we leverage the rich locational data provided by a origin-destination survey (Encuesta Origen Destino (EOD)) conducted in 2012 to explore disparities in exposure to particulate matter across income levels in Santiago, Chile. We merge the EOD data with course particulate matter (PM_{10}) and fine particulate matter ($PM_{2.5}$) concentrations from Santiago's network of air quality monitoring stations (SINCA) operated by the Ministry of the Environment of Chile (MMA). We focus on particulate matter air pollution because it leads to a broad range of severe health and non-health impacts and it drives the declaration of critical air quality episodes.

We find that individuals in lower-income deciles are exposed to higher concentrations of PM_{10} and $PM_{2.5}$ both when we assume that all individuals remain at their residential location 24 hours a day and when considering all locations reported on the reference day

of the EOD survey. Furthermore, in this context, the exposure gradients across income deciles for these two measures of exposure are similar.

Second, we evaluate the effect of a command-and-control air pollution policy on air quality. When government authorities expect spikes in particulate matter, they declare a critical air quality episode with the goal of reducing peak air pollution concentrations in the short-term. These episodes activate temporary (24 hour) restrictions, including prohibitions on driving a share of light-duty private vehicles based on the last digits of their license plates. These place greater restrictions on driving high emissions vehicles and impose new temporary restrictions on lower emissions vehicles.

During our period of analysis, the declaration of a critical air quality episode was based on the value of a city-wide air pollution index derived from PM_{10} concentrations measured at stations in the monitoring network. While the criteria for declaring an episode has discrete thresholds, in practice there are numerous determinants of critical air quality episodes. Therefore, we use a fuzzy regression discontinuity design to evaluate the effect of critical air quality episodes on air pollution concentrations. We find little evidence of a significant effect of the declaration of an episode on city-wide air quality.

Using the same fuzzy regression discontinuity design, we estimate heterogeneous effects of the critical air quality episodes across stations in the air quality monitoring network and across hours of the day. We find that the city-wide results mask significant heterogeneity. The declaration of an episode increases or has no significant effect on air pollution concentrations for most stations located in lower socioeconomic status neighborhoods, while it decreases air pollution concentrations at stations located in higher socioeconomic status neighborhoods.

Our paper contributes to the literature that evaluates the effects of policies to control pollution through short-term restrictions on driving and/or industry in Latin America (Aguilar-Gomez, 2025; Rivera, 2021; Mullins and Bharadwaj, 2015). Our paper is most similar to Rivera (2021), which documents the impacts of the critical air quality episodes on car trips, mass transit trips and air quality in Santiago. Following a similar empirical strategy, we find similar, but statistically insignificant, effects of the critical air pollution episodes on particulate matter. We extend these results by investigating the effects across

monitoring stations to uncover spatial heterogeneity in impacts.

Our paper also contributes to a burgeoning literature on the distributional impacts of environmental quality and policies to improve air quality (Banzhaf et al., 2019). Currie et al. (2023) documents that the Clean Air Act in the United States accounts for 60% of the racial convergence of PM2.5 pollution exposure in the United States since 2000. Similarly, Sager and Singer (2025) find that the 2005 Clean Air Act regulation of PM2.5 reduced PM2.5 levels, with larger decreases in more polluted areas, and that the regulation narrowed the Urban-Rural and Black-White PM2.5 exposure disparities. Hernandez-Cortes and Meng (2023) find that California's carbon market narrowed gaps in particulate matter between disadvantaged communities and other communities. Finally, Basaglia et al. (2025) find that a fuel taxation policy in Germany leads to larger reductions in air pollution emissions in low-income regions.

The remainder of the paper proceeds as follows. Section 2 provides context and section 3 describes the data that we use in this paper. Section 4 describes the methodology that we use to explore exposure to particulate matter across income deciles and the results that we find. Section 5 describes the empirical strategy that we use to identify the impacts of critical air quality episodes on air quality, the impacts that we find at the city-level and across monitoring stations, and a simple, back-of-the-envelope approximation of the impact of critical air quality episodes on the air pollution exposure of a representative individual from each income decile. Finally, section 6 concludes.

2 Context

Santiago is the most populous city in Chile with approximately 6 million residents (40% of the population of Chile). The Metropolitan Area of Santiago region is also the economic hub of Chile, contributing nearly half of the nation's gross domestic product (Trujillo et al., 2016). The region's principal tradable economic sectors are manufacturing, business and financial services, and transportation and communications (Trujillo et al., 2016). The non-tradable sector is concentrated in health and education (Trujillo et al., 2016).

Santiago is located in the flat basin of the Maipo River surrounded by high mountain

ranges, which hinder the free movement of polluting particles (Toro et al., 2019; Mazzeo et al., 2018). This effect is more pronounced in winter, when the wind system is weaker, leading to a weaker circulation of polluting particles (Mazzeo et al., 2018). At the same time, air pollution is also linked to thermal inversions, which is directly related to low temperatures and surface heating of the city (Toro et al., 2019). In the summer, atmospheric conditions can disperse pollutants more effectively (Gramsch et al., 2006), but occasionally summer particulate matter concentrations can match or surpass winter concentrations during periods of extensive forest fires in the region (de la Barrera et al., 2018).

Critical air pollution episodes are enacted during winter with the goal of improving the city's air quality. When critical air pollution episodes occur, several key restrictions are implemented to mitigate the high concentration of air pollution. These include limiting road usage for public transportation, imposing vehicle restrictions, banning agricultural burning, prohibiting the operation of cargo vehicles, and enforcing limitations on heating system usage. These measures are designed with the goal of managing and reducing air pollution levels during critical times. All of the Metropolitan Area of Santiago region is affected by the air quality episode restrictions except the commune of Talagante.

We focus on particulate matter air pollution, which drives the declaration of critical air quality episodes and has severe health impacts. Particulate matter is a mixture of solid particles and liquid droplets of different shapes, sizes, and chemical compositions. PM_{10} and $PM_{2.5}$ are two of the most commonly monitored types of particulate matter. PM_{10} refers to inhalable particulate matter with a diameter of less than 10 μm, and $PM_{2.5}$, a subset of PM_{10}, refers to fine particulate matter with a diameter of less than 2.5 μm. In many cities, PM_{10} has a longer history of ambient monitoring than other types of particulate matter (Southerland et al., 2022; Riojas-Rodriguez et al., 2016). However, $PM_{2.5}$ is likely the most studied type of particulate matter (see for example, Aguilar-Gomez et al. (2022); Sharma et al. (2020); Yuan et al. (2019)) because of the broad range of severe health impacts caused by exposure to it (Bell et al., 2004; Pope and Dockery, 2006). Furthermore, $PM_{2.5}$ is difficult to avoid because it permeates buildings more easily than PM10 (Tracy and Layton, 1995; Vette et al., 2001; Pope and Dockery, 2006; CARB, 2021).[2]

[2]https://ww2.arb.ca.gov/resources/inhalable-particulate-matter-and-health

Exposure to ambient particulate matter leads to morbidity and mortality (WHO, 2021; Wei et al., 2020; Schwartz et al., 2018; Baccini et al., 2017; Brook et al., 2010; EPA, 2009). Long-term exposure to ambient particulate matter is causally linked to cardiovascular and respiratory disease and mortality (Anderson et al., 2011; Cesaroni et al., 2014; Crouse et al., 2015) and short-term exposure to high levels of ambient particulate matter is causally linked to acute bronchitis, asthma attacks, increased susceptibility to respiratory infections, and worsened heart conditions, on the day of exposure and the following days (New York State Department of Health, 2021; EPA, 2010; Lin et al., 2002; Tertre et al., 2002). Exposure to particulate matter also negatively impacts labor productivity (Adhvaryu et al., 2022; Chang et al., 2016), labor supply (Hoffmann and Rud, 2024; Aragón et al., 2017), test scores (Bedi et al., 2021; Ebenstein et al., 2016), and decision-making and crime (Herrnstadt et al., 2021; Burkhardt et al., 2019; Sager, 2019).

3 Data

We use data from four principal sources. First, we collected hourly data on air pollutant concentrations, temperature and wind speed for each monitoring station in Santiago's air quality monitoring system (SINCA) operated by the Ministry of the Environment (MMA). Second, we use data on precipitation from the National Water Information System (SNIA). Third, we use data on the declaration of air quality episodes from the MMA of Chile. Fourth, we use data on surveyed individuals' income, educational attainment, and locations for a typical day from the Survey of Origin and Destination (Encuesta Origen Destino EOD) conducted by the Urban Transport and Road Infrastructure Program (SECTRA) in 2012. The following subsections will describe each of these data sets in more detail.

We focus on the time period 2009-2015 because the data on the declaration of air quality episodes is not available before 2009 and the criteria for declaring an air quality episode changed after 2015. Before 2015, general air quality episodes were declared. After 2015, the declaration of episodes was divided into specific episodes of PM10 or PM2.5.

3.1 Pollutants and Weather Data

The Metropolitan Area of Santiago has 11 real-time monitoring stations that record hourly concentrations of different pollutants and meteorological variables. Figure 1 plots the location of all monitoring stations in the Metropolitan Area of Santiago and the population density of each geographic unit, known as *comunas*. The figure also includes a 5 km buffer around each monitoring station to visualize the coverage of air quality monitoring in our analysis. The stations are distributed throughout the metropolitan region, with the Talagante commune located farther from the rest. We exclude Talagante and its monitoring station from our analysis of the impacts of air quality episodes because, as mentioned above, the restrictions associated with critical air quality episodes do not apply to this commune.

Figure 1: Location of Monitoring Stations

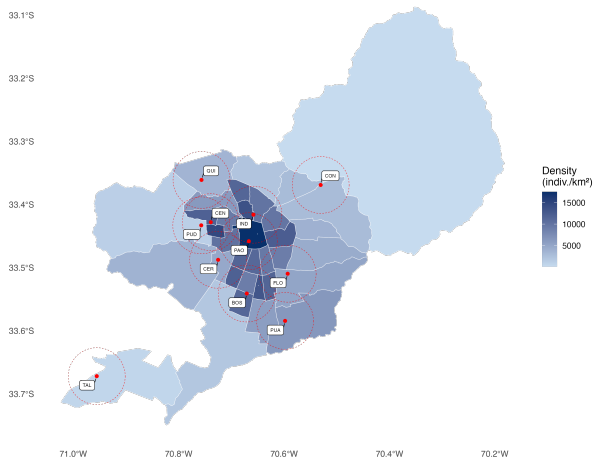

Notes: The figure shows the location of air quality monitoring stations in the Metropolitan Area of Santiago. The red dots represent the location of all active stations between 2009 and 2015. The figure also displays 5 km buffers around each station and the population density of each comuna, measured as population per square kilometer.

We use validated records from the monitoring network and spatially aggregate the air pollution data from the station-hour level to the location-hour level to create measures of the pollution concentration for each location-hour reported in the transport data as described in 4.1.

We also use the hourly data from the monitoring stations to construct the PM_{10} ICAP

variable following the MMA criteria to predict air quality episodes. Specifically, we build the PM_{10} ICAP variable according to the following procedure.

1. Using the hourly PM_{10} data from the monitoring stations, create 24-hour moving averages for the pollutant at all stations (separately).

2. Apply the MMA ICAP formula shown in equation 1 for each of the hourly 24-hour moving averages (separately for each station).

$$ICAP\ PM_{10} = \begin{cases} PM_{10} < 150 & : PM_{10} * \frac{2}{3} \\ PM_{10} \geq 150 & : PM_{10} * 2.22 - 233 \end{cases} \tag{1}$$

   where PM_{10} is the 24-hour moving average of PM_{10} at each station.

3. Calculate the daily maximum ICAP variable across stations and hours.

The procedure results in a variable capturing the maximum PM_{10} ICAP across stations at the Santiago-day level.

Table 1: Descriptive Statistics

Variables	Obs	Mean	Std. Dev.	Min	Max	Years
PM_{10} validated	61,344	67.48	40.04	1	445.50	2009-2015
$PM_{2.5}$ validated	61,344	27.52	18.76	1	265.55	2009-2015
Daily max. PM_{10} ICAP	61,344	77.43	54.02	13	495	2009-2015
Temperature (°C)	60,780	15.44	7.05	-2.21	35.59	2009-2015
Wind speed (m/s)	60,874	1.38	0.92	0.10	5.34	2009-2015
Precipitation	61,344	0.73	3.52	0	52.71	2009-2015

Notes: Descriptive statistics for pollution and weather variables in the Metropolitan Area of Santiago region, excluding the monitoring station of Talagante.

Table 1 presents descriptive statistics for the air pollution and weather variables used in our fuzzy regression-discontinuity design. The mean of the validated hourly PM_{10} observations across all stations (excluding Talagante) is 67 $\mu g/m^3 N$ and the mean of the validated hourly $PM_{2.5}$ observations across all stations (excluding Talagante) is 27 $\mu g/m^3$. These values are above the WHO's short-term (24-hour) air quality guidelines for PM_{10}

(45 $\mu g/m^3$) and $PM_{2.5}$ (15 $\mu g/m^3$). The mean of the daily max PM_{10} ICAP is 77, which is substantially below the threshold of 200 for declaring a critical air quality episode (see section 3.2).

3.2 Air Quality Critical Episodes Data

Table 2 shows the number of air quality episodes declared from 2009-2015. There are three types of episodes: alerts, pre-emergencies, and emergencies. The air quality level is in an "Alert Phase" if the Air Quality Index for Particulate Matter (ICAP) is between 200-299, in a "Pre-emergency Phase" if the ICAP is between 300-499, and in an "Emergency Phase" if the ICAP is 500 or above. Episodes are declared in winter months from April 1 to August 31 (MMA, 2015). Across the years in our sample, there are 8 to 55 episodes declared annually. The sample does not contain any declarations of emergencies, and pre-emergency declarations account for 0 - 39% of the episodes depending on the year.

Table 2: Number of Air Quality Episodes from 2009 to 2015

Year	Alerts	Pre-emergencies	Emergencies	Total
2009	23	0	0	23
2010	11	2	0	13
2011	18	7	0	25
2012	23	2	0	25
2013	8	0	0	8
2014	22	1	0	23
2015	50	5	0	55

Note: This table presents the number of air quality episodes declared from 2009-2015. Episodes are divided between alerts, pre-emergencies, and emergencies. The data source for the air quality episodes is the MMA.

3.3 Survey of Origin and Destination

The Origen Destination Survey (Encuesta Origen Destino) was collected by SECTRA in 2012. SECTRA is a government program under the Undersecretariat of Transport of the Ministry of Transport and Telecommunications (MTT) of Chile. It is a technical agency specialized in transport planning. The EOD is conducted for each region of Chile. The household survey sample is randomly selected. First, a block is selected and then house-

holds within that block are chosen to be surveyed. The data is collected through two face-to-face visits.

For households participating in the EOD, each member of the household provides detailed information on all trips taken on the assigned "Travel Day" (the reference day), which is determined in agreement with the head of household. During the first visit, a surveyor records household and individual characteristics such as the number of household members, family relationships, educational level, current occupation, number and type of motorized vehicles and/or bicycles, and income data. The surveyor also provides each household member with a form called a "General Travel Log" where each person records all trips taken—whether on foot or using any means of transportation—on the assigned "Travel Day,". During the second visit, the surveyor conducts personal interviews with each household member and records all trips taken by each person using the information provided in the "General Travel Log". The surveyor enters the data into the survey software, which records the responses to questions regarding the trips made on the assigned "Travel Day".

To understand Santiago residents' air pollution exposure at their home and at all the locations they visit during the reference day, we match the individual-location data from EOD with the spatially aggregated air pollution data for 2012, the year in which the survey was conducted.

4 Exposure to Air Pollution

4.1 Methodology

We leverage the rich locational data provided by an origin-destination survey (Encuesta Origen Destino (EOD)) conducted in 2012 to explore disparities in exposure to particulate matter across income levels in Santiago, Chile. We merge the EOD data with course particulate matter (PM10) and fine particulate matter (PM2.5) concentrations from Santiago's network of air quality monitoring stations (SINCA) operated by the Ministry of the Environment of Chile. We focus on particulate matter air pollution because it drives the

declaration of critical air quality episodes.

Using the EOD data, we construct two exposure measures—one based on each individual's residential location and another based on all locations that an individual reported visiting on the reference day of the EOD survey. The residential exposure measure assumes that each individual in our sample remains at their residence for all 24 hours of the reference day. The all-locations measure uses each individual's hourly reported geocoordinates to determine their pollution exposure at each hour of the reference day. Residential coordinates are inferred from "return home" trips; when a respondent does not report a "return home" trip, we use a household member's "return home" trip to determine the residential location, and if no household members report a "return home" trip, then we use the first reported origin as the residential location.

We construct our sample of individuals in two steps: (i) restrict the sample to individuals who's residential location and all locations reported on the reference day are within 5 km of at least one monitoring station (for robustness, we also consider a 20 km radius); (ii) restrict the sample to adults aged 25+. We observe or infer the residential location for roughly 75% of individuals aged 25+.

To generate measures of annual PM2.5 and PM10 exposure, we assume an individual's hourly locations for every day of 2012 are the same as those on the reference day. Then, we aggregate the 11 stations' hourly pollutant concentrations to each reported location. The pollutant concentration for each location-hour is calculated using an inverse-distance-squared (i.e. inverse quadratic) average of stations within 5 km (or within 20 km for robustness), reweighting over stations that actually report the pollutant concentration for that hour so that missing observations do not bias calculated concentrations downward. The annual exposure is the average of these hourly exposures over the full year. See Appendix 3.2 for methodological details.

Our sample restrictions ensure that the residential and all locations exposure measures are defined for the same sample of individuals, and that, in the absence of missing hourly air pollutant data from monitoring stations, we have a balanced panel at the individual-hour level. Using a smaller radius around stations provides a more accurate measure of the pollution concentration at a given location and it results in more variation in pollutant

concentrations across locations, but it also limits the size of our sample because fewer individuals are covered by air pollution data. Using a 5 km radius around monitoring stations, 48.97% of the individuals aged 25+ in the EOD data (i.e. 18,940 individuals) are included in our sample. Expanding the radius to 20 km around stations, 68.9% of individuals in the EOD data aged 25+ are included. Income deciles are created using per-capita household income (household income divided by the number of household members) as reported in the EOD data.

4.2 Results

Figure 2 shows annual mean PM2.5 and PM10 residential and all locations exposure across income deciles. Appendix Figure B.2 shows the exposure measures across income deciles using a 20 km radius. Annual PM2.5 exposure is similar across the lower five income deciles before decreasing over the upper five deciles. For PM2.5, although the annual residential exposure is slightly below the annual all locations exposure, the two measures of exposure are very similar for all deciles. Annual PM10 exposure is similar across the lower seven deciles and then decreases over the upper three deciles. In the case of PM10, the all locations exposure is above the residential exposure, although the confidence intervals overlap.

Two types of descriptive statistics may help to explain these results. First, Appendix tables A.1 and A.2 display the shares of individuals in our sample working (defined as the location different from their residence where the individual spends the greatest number of hours on the reference day) and residing nearest to each station by income decile. For many income deciles, the share of individuals living and working nearest to each station is similar. Few individuals reside or work nearest to the TAG station. Second, most stations, except CON, display similar patterns of particulate matter concentrations across hours of the day (see Appendix figure B.3). Furthermore, with the exception of the CON and TAL stations, the average PM2.5 and PM10 concentration is similar across stations at each hour of the day. Therefore, aggregating across all individuals in an income decile can lead to similar results for both measures of exposure.

Figure 2: Mean Exposure to PM2.5 and PM10 in 2012 Using a 5 km Radius, by Income Deciles

(a) PM2.5 Mean

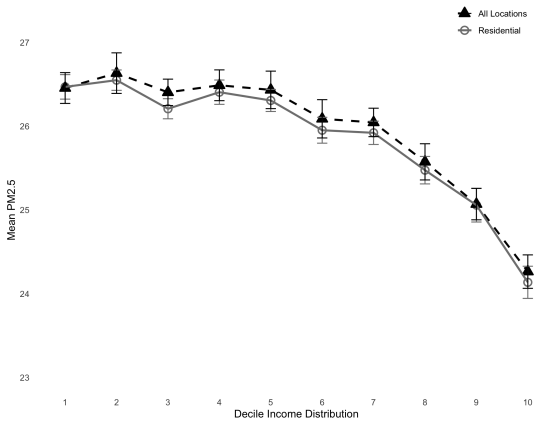

(b) PM10 Mean

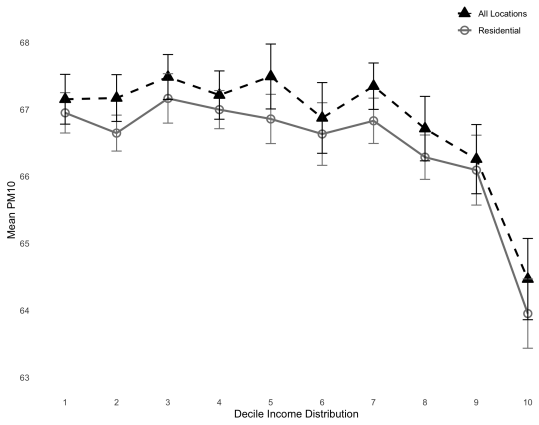

Source: Encuesta Origen - Destino a Hogares (EODH), 2012; pollution data from SINCA, 2012.

Notes: This figure plots annual mean exposure to PM2.5 and PM10 across income deciles using a 5 km radius around monitoring stations. "Residential" refers to the exposure measured at an individual's residence as reported in the survey. "All locations" represents the individual's actual location during the reference day as reported in the EOD survey. Exposure values are computed using inverse quadratic distance weighting from all monitoring stations within the specified radius. Individuals are included in the sample if all of their locations reported during the reference day are within 5 km of a monitoring station and they are at least 25 years old. Sampling survey weights are applied.

5 Impact of Air Pollution Critical Episodes on Air Pollution Concentrations

5.1 Empirical Strategy

We employ a Fuzzy Regression Discontinuity Design (RDD) to estimate the impact of air quality critical episodes on pollution measures in winter months (i.e. April 1 to August 31) when episodes are declared. The fuzzy RDD is particularly suited to scenarios where the treatment, the declaration of an air quality critical episode in this case, is not perfectly assigned based on the running (i.e. assignment) variable.

Our running variable is the daily maximum PM_{10} ICAP across stations in $t-1$. We built this variable following the MMA criteria described in Section 3.1. In this section, the notation for our running variable is $\bar{x}_{t-1}$. The rationale for using the daily maximum ICAP in $t-1$ is that it serves as a predictor of the probability that a critical air quality episode will be declared on the following day t.[3] Figure 3 plots the daily maximum PM_{10} ICAP level and the days with a declared episode during winter 2015. This figure illustrates that there were days with the daily maximum PM_{10} ICAP below the alert threshold in which an alert episode was declared.[4] Therefore, while the air quality episode thresholds can predict the declaration of an episode, they are not perfect predictors.

Figure 3: Episodes and Daily Maximum ICAP PM10 (2015)

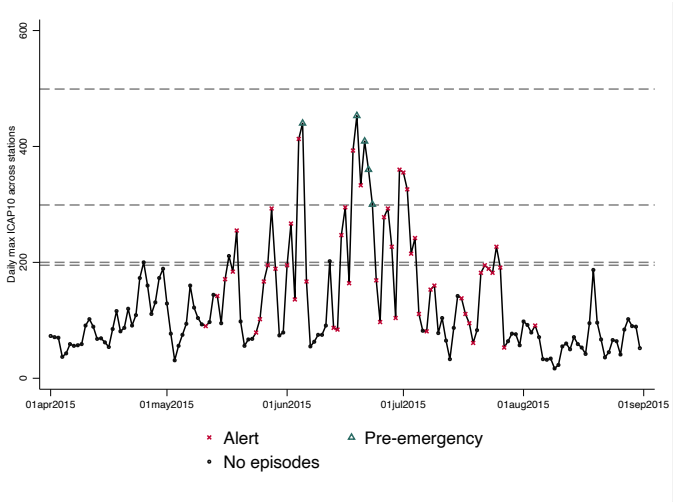

Notes: This figure plots the daily maximum PM_{10} ICAP level in day t and the days with restrictions (i.e. episodes) on day t during winter 2015. The daily maximum PM_{10} ICAP was built following the MMA criteria described in Section 3.1.

Source: Data on PM10 levels were collected from SINCA and data on air quality episodes from MMA.

[3]Critical air quality episodes are declared in the evening the night before the restrictions take place. We denote a critical air quality episode on day t to be an episode declared the evening of day $t-1$ with resetrictions that take place on day t.

[4]Appendix Figure B.1 plots the PM_{10} ICAP level and the days with a declared episode during the winters of 2009-2014.

5.1.1 City-wide specification

We first partial out controls from our daily outcomes by estimating the following equation:

$$y_t = \alpha + \beta' W_{t,t-1} + \mu' \text{FE}_t + \pi\, T_{t-1} + u_t, \tag{2}$$

where y_t represents the daily mean of PM10 or PM2.5 across all monitoring stations (in logs). $W_{t,t-1}$ is a vector of weather-controls (precipitation, temperature, wind speed, and the daily maximum to minimum temperature range ΔR_t) and their squares in day t and day $t-1$s.[5] FE_t denotes a set of time fixed effects including year, month, day of week, and weekend fixed effects. T_{t-1} is an indicator if there was a declaration of a critical air quality episode the day before (i.e. restrictions were in place on day $t-1$). From this regression, we obtain the residuals $\hat{r}_t$. Each outcome in the fuzzy RDD is its residualized version, $\hat{r}_t$. In all our specifications, we calculate and use the optimal bandwidth (b) for each daily outcome following Calonico et al. (2020).

The first stage of our fuzzy RDD involves determining the likelihood that a critical air quality episode is declared. Equation 3 shows our specification for the first stage:

$$T_t = \alpha_0 + \alpha_1 1[\bar{x}_{t-1} \geq 0] + \alpha_2 \bar{x}_{t-1} + \alpha_3 \{1[\bar{x}_{t-1} \geq 0] \times \bar{x}_{t-1}\} + \alpha_4' W_{t,t-1} + \alpha_5' \text{FE}_t + \alpha_6\, T_{t-1} + \epsilon_t \tag{3}$$

where the treatment variable T_t is defined as an indicator of whether there was an episode with restrictions on day t. $\bar{x}_{t-1}$ is the daily maximum PM_{10} ICAP across stations in $t-1$, and $1[\bar{x}_{t-1} \geq 0]$ is an indicator variable for whether the daily maximum PM_{10} ICAP is above the lowest threshold for declaring an episode (ICAP = 200). We normalize our running variable relative to the threshold for declaring an episode (ICAP=200).

In the second stage, we assess the impact of critical air quality episodes on Santiago's overall air quality levels. Our specification is as follows:

$$\hat{r}_t = \beta_0 + \beta_1 \hat{T}_t + \beta_2 \bar{x}_{t-1} + \beta_3 (\hat{T}_t \times \bar{x}_{t-1}) + \eta_t \tag{4}$$

[5] We include the t and $t-1$ subscripts in $W_{t,t-1}$ to indicate that weather controls are included for the contemporaneous day (t) and the previous day ($t-1$). The variable ΔR_t serves as a proxy for the presence of a thermal inversion at the daily level.

where $\hat{r}_t$, T_t, and $\bar{x}_{t-1}$ are defined as described above.

Moreover, following Rivera (2021), for our estimation strategy, we use a two-step efficient Generalized Method of Moments (GMM-IV) approach with small-sample robust standard errors. This procedure accounts for serial correlation in the data. This is performed with the Newey-West heteroskedastic- and autocorrelation-consistent HAC weighting matrix.[6]

We use data from the winter months (April through August), when critical air quality episodes are declared (MMA, 2015) in our main results. This seasonal focus ensures that our results capture the effects of the declaration of episodes. In Appendix Sections A and B, we show results using all calendar months to verify robustness.

5.1.2 Station-level specification

We employ a fuzzy RDD analysis at the station level to explore differential impacts of critical air quality episodes across neighborhoods. Let $s \in \{1, \ldots, 10\}$ index monitoring stations and t index time. At the daily frequency, our outcome is y_{st}, and at the hourly frequency, our outcome is y_{sht}. The running variable is the same for all stations. Because critical air quality episodes are declared at the city level, we use the same running variable, the daily maximum PM_{10} ICAP across stations in $t-1$, as in our city-wide specification. RD samples are restricted to the optimal bandwidth for each outcome at the city-wide level. For our station-level specification, we use daily and hourly station data. Precipitation and daily max-min temperature range are measured at the daily city-wide level, while temperature and wind speed are measured at the station level.

Let $W_{st,t-1}$ be the weather-control vector for station s on day t. We include contemporaneous levels and their squares for precipitation, temperature, wind speed, and the daily max–min temperature range ΔR_t. We also include one-day lags and their squares for precipitation, temperature, wind speed, and ΔR_t. In addition, we include year, month, day of week, weekend fixed effects (FE_t) and an indicator if there was an episode declared the prior day T_{t-1}.

[6]The covariance uses a Bartlett (triangular) kernel with bandwidth 1, i.e., a HAC/Newey–West–type estimator that linearly down-weights serial covariances by lag and truncates them at lag 1 so only contemporaneous and first-lag correlations enter.

Two-Step Estimator: Residualization and Fuzzy RDD (Daily)

Step 1 (station-specific residualization). For each station s, we first partial out controls from the daily outcome by OLS:

$$y_{st} = \alpha_s + \beta_s' W_{st} + \mu_s' \text{FE}_t + \pi_s \, T_{t-1} + u_{st}, \tag{5}$$

where W_{st}, FE_t, and T_{t-1} are defined as described above. From this regression, we obtain the residuals $\hat{r}_{st}$.

Step 2 (station-level fuzzy RDD). In the RD sample for each outcomes, we estimate the following for each station s

$$\hat{r}_{st} = \gamma_{0s} + \tau_s \, \hat{T}_t + \gamma_{1s} \, (\bar{x}_{t-1} \times \hat{T}_t) + \gamma_{2s} \, \bar{x}_{t-1} + \varepsilon_{st}. \tag{6}$$

This is analogous to Equation 4 in the city-wide specification, but estimated separately for each station s. The coefficient of interest, τ_s, captures the station-specific daily effect of critical episode declarations. We estimate this equation separately for PM10 (using the city-wide optimal bandwidth $b = 69.86$) and $PM_{2.5}$ (using the city-wide optimal bandwidth $b = 70.71$).

Two-Step Estimator: Residualization and Fuzzy RD (Hourly)

Step 1 (station-specific residualization). For each station s, we consider each station's hourly panel separately and partial out controls from the hourly outcome by OLS:

$$y_{sht} = \alpha_{sh} + \beta_{sh}' W_{st} + \mu_{sh}' \, \text{FE}_t + \pi_{sh} \, T_{t-1} + u_{sht}, \tag{7}$$

using the weather-control vector $W_{st,t-1}$, the time fixed effects FE_t and T_{t-1} indicating that a critical air quality episode with restrictions was in place on day $t-1$. From this regression, we obtain hourly residuals $\hat{r}_{sht}$.

Step 2 (hour-specific station-level fuzzy RDD). For each station and each hour of the day $h \in \{0, \ldots, 23\}$, we restrict the sample to the city-wide optimal bandwidth and estimate

$$\hat{r}_{sht} = \gamma_0 + \tau_{sh} \, \hat{\text{T}}_t + \gamma_1 \, (\bar{x}_{t-1} \times \hat{T}_t) + \gamma_2 \, \bar{x}_{t-1} + \varepsilon_{sht} \qquad \forall \, h \in \{0, \ldots, 23\}, \tag{8}$$

which is again analogous to Equation 4, but estimated separately for each station s and hour h. The coefficient of interest is τ_{sh}, the hour-specific effect for station s. We estimate this separately for PM10 (using the city-wide optimal bandwidth $b = 69.86$) and $PM_{2.5}$ (using using the city-wide optimal bandwidth $b = 70.71$). As in the city-wide analysis, our baseline station-level results are estimated for the winter months. Appendix Sections A and B present corresponding estimates using data from all calendar months.

5.2 First Stage

Table 3 shows the results for the first stage of the fuzzy RDD using daily data. Column (1) shows the coefficient for $ICAP10_{t-1} \geq 0$ when the second-stage outcome is the $PM10_{10}$ mean. Column (2) shows the coefficient for $ICAP10_{t-1} \geq 0$ when the second-stage outcome is the $PM_{2.5}$ mean.[7] For each specification, we report the first-stage F statistic and the value of the optimal bandwidth. Table 3 results suggest that the probability of an episode being declared on day t increases when $ICAP_{10_{t-1}}$ exceeds the 200 threshold.

Table 3: First Stage Results – Daily Data

	(1)	(2)
	Probability of an episode in day t	
Second stage outcome	*PM_{10} mean*	*$PM_{2.5}$ mean*
$ICAP10_{t-1} \geq 0$	0.286**	0.286**
	(0.130)	(0.130)
Observations	188	188
Weather controls	✓	✓
F statistic	13	13
Bandwidth	Optimal = 69.86	Optimal = 70.71

Notes: This table reports the first stage results for our fuzzy regression discontinuity design using daily data for winter months. See Section 5.1.1 for a detail description of the city-wide specification. The running variable is the daily maximum ICAP for PM 10 on day $t-1$. The first stage dependent variable is a dummy for whether there was an episode with restrictions on day t. The corresponding second stage outcome differs across columns. The second stage outcome is the daily mean PM_{10} in column (1) and the daily mean $PM_{2.5}$ in column (2). Each column uses a different bandwidth around the normalized cutoff ($c = 0$). Columns (1) and (2) uses the optimal bandwidth following Calonico et al. (2020). Robust standard errors in parentheses. * $p < 0.1$, ** $p < 0.05$, *** $p < 0.01$.

Moreover, Figure 4 illustrates the first-stage of our fuzzy RDD. This figure shows that

[7] $ICAP10_{t-1} \geq 0$ is our running variable normalized to zero. Therefore, the cutoff for the RDD specification is zero.

the likelihood of declaring an air quality episode increases with the running variable and that there is a discrete jump in the likelihood of declaring an episode at the cutoff. The plot displays binned means of the fitted probability that an air quality episode is declared as a function of the running variable. The fitted values come from a regression of episode declarations on a full set of weather controls, an indicator of whether the day before an episode was declared, and time fixed effects. Separate local linear fits are shown on each side of the cutoff using a triangular kernel. Following Calonico et al. (2020), we will focus on the estimates using the optimal bandwidth in the second stage.

Figure 4: First Stage RD plot

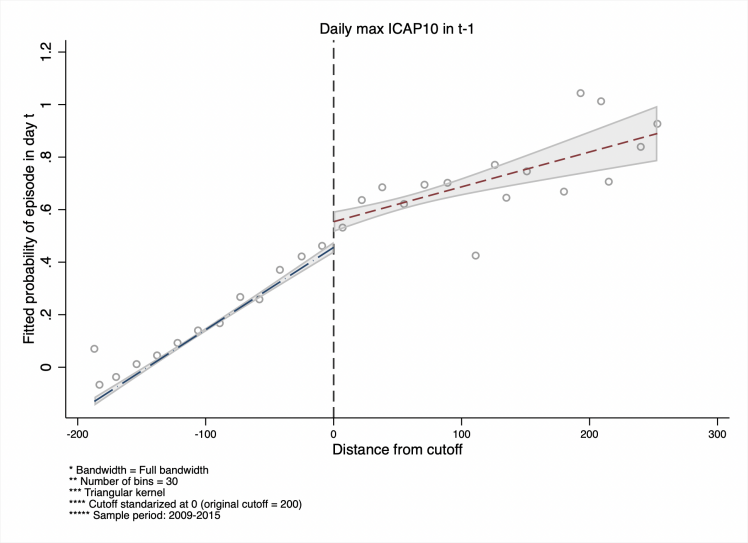

Notes: This figure plots the first stage of the fuzzy regression discontinuity design. The running variable is the daily maximum $ICAP10_{t-1}$, normalized so that zero marks the cutoff for declaring an air quality episode. Each circle represents the binned mean of the fitted probability that there was an episode with restrictions in place on day t, conditional on $ICAP10_{t-1}$. The fitted values come from a regression including weather controls, an indicator if the day before an episode was declared, and time fixed effects. Separate local linear fits are estimated on each side of the cutoff using a triangular kernel. The gray region displays 90% confidence intervals.

5.3 Results

5.3.1 City-Wide Results

Table 4 reports the results of the second stage of the fuzzy RDD at the city level using daily data. Across different measures of PM_{10} and $PM_{2.5}$ at the daily level, we do not see a consistent significant effect of the critical air quality episodes on city-wide daily particulate matter measures. However, we do find a statistically significant and negative

effect of episodes on $PM_{2.5}$ mean concentrations during daytime and early evening hours (8am–8pm).

Table 4: City-Wide Second Stage Results: Daily Data

	PM_{10}			$PM_{2.5}$		
	Mean	Max	Mean 8am-8pm	Mean	Max	Mean 8am-8pm
$\hat{P}(\text{episode}_t)$	-0.039	-0.027	-0.066	-0.042	0.035	-0.095**
	(0.036)	(0.057)	(0.040)	(0.038)	(0.054)	(0.043)
Observations	188	169	181	188	173	195
Weather controls	✓	✓	✓	✓	✓	✓
Outcome mean	4.34	5.55	4.35	3.56	4.71	3.45
Optimal bwd	69.83	63.83	67.13	70.71	66.34	71.29

Notes: This table reports the city-wide second stage results for our fuzzy regression discontinuity design using daily data for winter months. See Section 5.1.1 for a detail description of the city-wide specification. All columns report the results using the optimal bandwidth for each outcome.

5.3.2 Station-Level Results

We explore heterogeneity in the effects of critical air quality episodes across different locations in Santiago. To do this, we estimate our main specification for each station separately. The results are shown in Table 5. The daily running variable continues to be $\bar{x}_{t-1}$ at the city-level for each station-level specification based on the criteria for declaring a critical air quality episode. Therefore, all stations have the same main predictor variable in the first stage. In the second stage, the outcome is the daily mean pollutant concentration at each station.

The station-level results provide evidence of heterogeneity in the effect of critical air quality episodes. The results shown in Table 5 are ordered by station elevation, from lowest to highest. The highest-elevation station experiences a statistically significant reduction in both pollutant concentrations, PM_{10} and $PM_{2.5}$, following the declaration of an episode. This station is also located in the highest socioeconomic status neighborhood, proxied in Table 5 by the mean education level of the census geographic area where the monitoring station is located. Moreover, stations such as IND and PAO, located in the city center and in more densely populated areas (see Figure 1), also exhibit reductions in mean $PM_{2.5}$ concentrations when an episode is declared. However, the magnitude of the effect is substantially larger for the station located in the highest socioeconomic status area according to this criteria.

Table 5: Daily Effect of a Critical Episode on PM_{10} and $PM_{2.5}$, by Station

	QUI		PUD		CEN		CER		IND		PAO		BOS		FLO		PUA		CON	
	PM10	PM2.5	PM10	PM2.5	PM10	PM2.5	PM10	PM2.5	PM10	PM2.5	PM10	PM2.5	PM10	PM2.5	PM10	PM2.5	PM10	PM2.5	PM10	PM2.5
$P(\widehat{episode}_t)$	-0.030	-0.047	-0.026	-0.071	0.030	0.022	-0.022	0.020	-0.044	-0.085**	-0.046	-0.086**	0.033	0.022	0.001	-0.032	0.041	0.064	-0.121**	-0.217***
	(0.048)	(0.055)	(0.052)	(0.051)	(0.037)	(0.044)	(0.041)	(0.050)	(0.035)	(0.036)	(0.041)	(0.041)	(0.043)	(0.058)	(0.040)	(0.048)	(0.047)	(0.055)	(0.052)	(0.057)
Elevation	491	491	491	491	500	500	513	513	553	553	558	558	580	580	606	606	672	672	799	799
Mean education level (census geographic area)	10.489	10.489	10.186	10.186	10.019	10.019	10.744	10.744	12.003	12.003	9.789	9.789	10.993	10.993	12.375	12.375	12.616	12.616	15.391	15.391
Observations	171	171	127	127	150	151	166	165	164	164	170	164	169	169	162	137	143	143	155	155
Outcome mean	4.459	3.529	4.349	3.616	4.375	3.697	4.325	3.595	4.283	3.491	4.388	3.532	4.415	3.651	4.411	3.553	4.169	3.446	3.940	3.186
Optimal bandwidth	69.83	70.71	69.83	70.71	69.83	70.71	69.83	70.71	69.83	70.71	69.83	70.71	69.83	70.71	69.83	70.71	69.83	70.71	69.83	70.71

Notes: This table reports the second stage results at the station-level following the empirical strategy described in Section 5.1.2, using daily data for winter months. All columns report the results using the optimal bandwidth at each side of the cutoff (c=0). This optimal bandwidth is set to be the same for all stations and comes from the optimal bandwidth at the city-wide daily level.

Figures 5 and 6 show that the station-level results are driven by differences in within-day patterns. Stations located neighborhoods with higher educational attainment, such as CON and IND, display statistically significant and negative coefficients for both PM_{10} and $PM_{2.5}$ across a larger share of hours, indicating that critical episodes are associated with reductions in local concentrations more consistently throughout the day. In contrast, stations in neighborhoods with lower educational attainment, such as CEN, PUD, QUI, and CER, exhibit much weaker improvements and, in several cases, near-zero or positive coefficients during evening and nighttime hours. Overall, the hourly estimates suggest that the benefits of critical episodes are concentrated in areas with higher educational attainment and that aggregate city-wide effects contain different spatial and temporal impacts.

Figure 5: Hourly Effect of a Critical Episode on PM_{10}, by Station

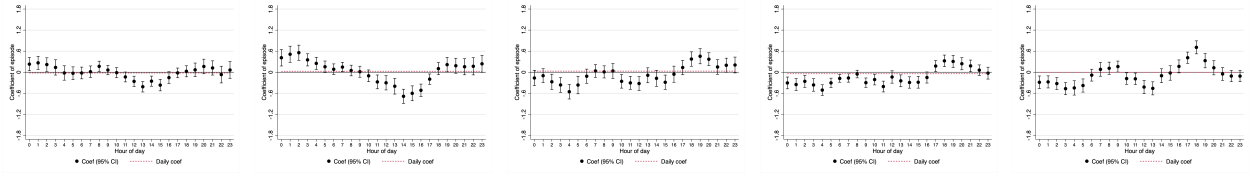

(a) CER (b) CEN (c) BOS (d) IND (e) FLO

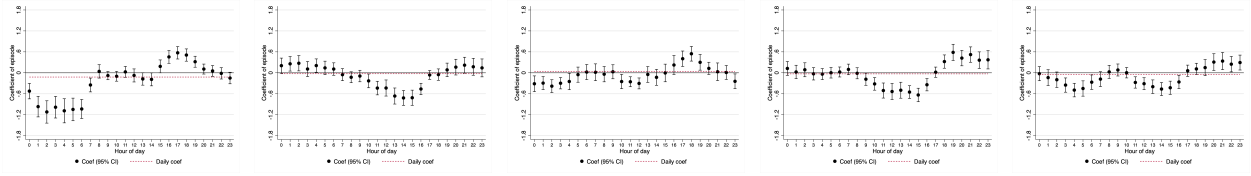

(f) CON (g) PUD (h) PUA (i) QUI (j) PAO

Notes: Each panel plots the second-stage results for PM_{10} for each station, following the empirical strategy described in Section 5.1.2 using hourly data for the winter months. All columns report the results using the optimal bandwidth on each side of the cutoff ($c = 0$). This optimal bandwidth is the same for all stations and is based on the optimal bandwidth estimated at the citywide daily level.

Figure 6: Hourly Effect of a Critical Episode on $PM_{2.5}$, by Station

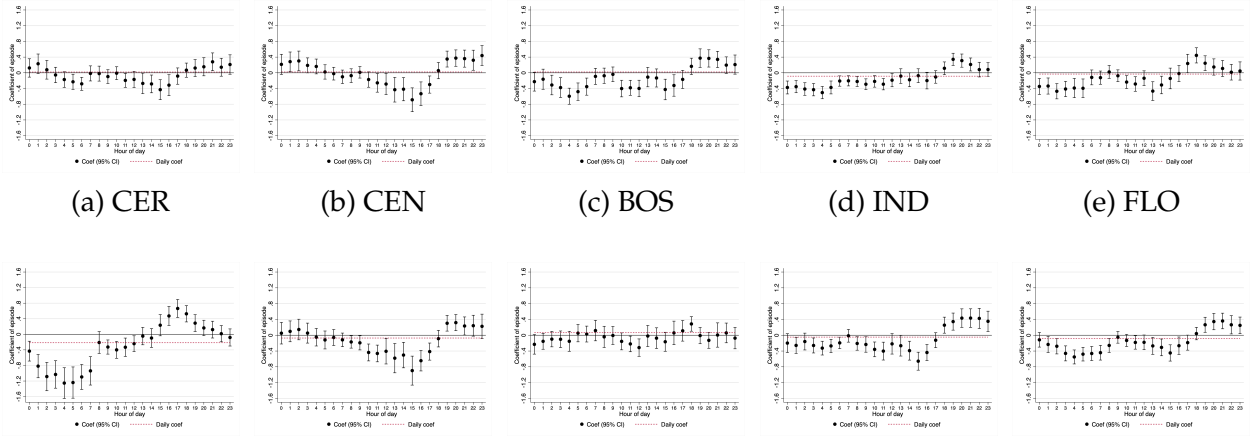

(a) CER (b) CEN (c) BOS (d) IND (e) FLO

(f) CON (g) PUD (h) PUA (i) QUI (j) PAO

Notes: Each panel plots the second-stage results for $PM_{2.5}$ for each station following the empirical strategy described in Section 5.1.2 using hourly data for the winter months. All columns report the results using the optimal bandwidth on each side of the cutoff ($c = 0$). This optimal bandwidth is the same for all stations and is based on the optimal bandwidth estimated at the citywide daily level.

Motivated by these results, we will further explore this heterogeneity in the next subsection. Specifically, we will analyze whether the heterogeneity in the effect of air quality episodes causes systematically different pollution exposure across income levels using the individual-level EOD data.

5.3.3 Individual-Level Analysis

We combine the RDD station-level estimates of the effect of critical air pollution episodes for each hour of the day with our individual-level EOD microdata to construct "representative individual" exposure profiles by income decile. For each decile, we identify the monitoring station where the largest share of individuals live (home station) and the station where the largest share work (work station),[8] using the information reported in Tables A.1 and A.2. We then link these residential and work locations to the hourly station-specific RDD coefficients for PM_{10} and $PM_{2.5}$. Each representative individual is assumed to be at home from 19:00–08:00 and at work from 09:00–18:00, so the 24-hour profile is built by stitching together, hour by hour, the relevant episode coefficients from the home

[8]Note that we define the work location as the non-residential location in which the individual reports spending the greatest number of hours in the reference day.

station (night and early morning) and the work station (daytime). Figures 7 and B.6 show income decile plots that summarize how critical episodes translate into different intra-day pollution responses across the income distribution given where individuals typically live and work.

Focusing on Figure 7, in the lowest decile (D1), the representative individual lives and works near station FLO. At this station, the coefficients are significantly negative from 00:00 to 05:00 and 10:00 to 13:00, indicating overnight, mid-morning, and early-afternoon improvements in local air quality on days in which an episode with restrictions was in place. During commuting hours (07:00 to 09:00 and 16:00 to 20:00), the coefficients are meaningfully positive, suggesting that D1 individuals are exposed to higher-pollution concentrations while commuting. Outside that window, coefficients remain close to zero in the early morning and become slightly positive in the late evening, suggesting limited—or even adverse—changes later in the day.

In the next lowest deciles (D2–D3), the representative individuals live near stations PUA and BOS and work near station IND. At these stations, the coefficients are significantly negative from roughly 09:00 to 16:00 and from 02:00 to 04:00. Outside these windows, coefficients remain close to zero and become slightly positive in the late evening.

By contrast, in the highest decile (D10), the representative individual resides and works near IND, where the coefficients are consistently negative and statistically significant for most of the day (approximately from 00:00 to 16:00) before turning positive only for a short late-afternoon and evening period (17:00 to 21:00).

For the upper-middle deciles (D8–D9), whose representative individuals primarily live near station FLO and work near station IND, the patterns closely resemble those observed for the highest decile (D10). In both D8 and D9, coefficients are consistently negative from 00:00 to roughly 06:00, indicating early-morning improvements in air quality very similar to those seen for D10. However, unlike the highest decile, representative individuals in D8 and D9 have small but positive coefficients between 07:00 and 08:00, suggesting higher pollution exposure during the morning commuting period. After this spike, coefficients return to mildly negative or near-zero values through the late morning and early afternoon.

Taken together, comparing the lower, upper-middle, and highest deciles reveals a socioeconomic gradient: as income rises, the timing and duration of pollutant reductions become longer and more stable. Lower-income groups benefit only within narrow time windows and may face greater exposure during commuting hours, whereas higher-income groups experience more sustained improvements over the day due to the spatial clustering of their homes and workplaces in areas where air-quality restrictions appear to be more effective.

Figure 7: Hourly effect of a critical episode on PM_{10} for representative individuals by income deciles

(a) Decile 1 (b) Decile 2 (c) Decile 3 (d) Decile 4 (e) Decile 5

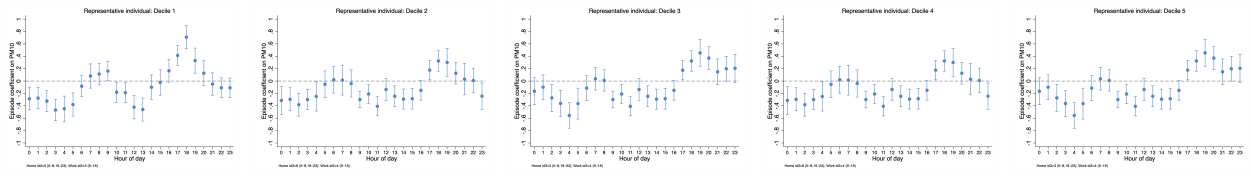

(f) Decile 6 (g) Decile 7 (h) Decile 8 (i) Decile 9 (j) Decile 10

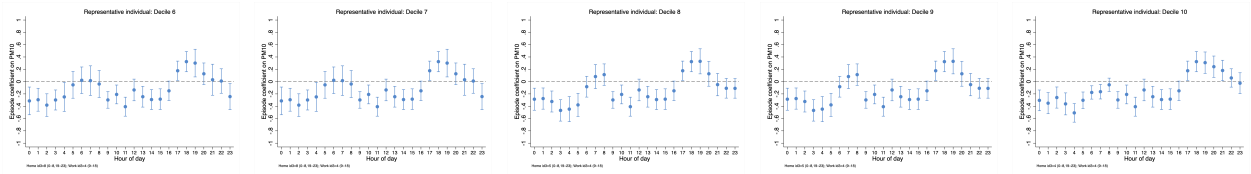

Notes: Each panel plots the second-stage results for PM_{10} at the station level for the representative individual of each income decile following the empirical strategy described in Section 5.1.2 using hourly data for the winter months. All columns report the results using the optimal bandwidth on each side of the cutoff ($c = 0$). This optimal bandwidth is the same for all stations and is based on the optimal bandwidth estimated at the citywide daily level.

6 Conclusion

We document that lower income individuals in Santiago, Chile are exposed to higher levels of PM10 and PM2.5 at their residential location and when taking into account their locations throughout the entire day. The exposure gradient across income deciles is similar for both measures of annual air pollution exposure. We use a fuzzy regression discontinuity design to document that the declaration of critical air quality episodes, which activate city-wide restrictions on private vehicles among others, has minimal effects on

overall air quality levels but has heterogeneous effects across space and hours of the day.

Our results have important implications for policy. Command-and-control policies may not be broadly effective at reducing spikes in air pollution and their effects may differ across neighborhoods. Considering the spatial and temporal impacts of city-wide policies could lead to improvements in health and well-being.

References

Adhvaryu, A., Kala, N., and Nyshadham, A. (2022). Management and shocks to worker productivity. *Journal of Political Economy*, 130:1–47.

Aguilar-Gomez, S. (2025). Adaptation and mitigation of pollution: Evidence from air quality warnings. *Journal of Environmental Economics and Management*, 134:103215.

Aguilar-Gomez, S., Dwyer, H., Zivin, J. G., and Neidell, M. (2022). This is air: The "non-health" effects of air pollution. *Annual Review of Resource Economics*, page 403–25.

Anderson, J., Thundiyil, J., and Stolbach, A. (2011). Clearing the air: A review of the effects of particulate matter air pollution on human health. *Journal of medical toxicology: official journal of the American College of Medical Toxicology*, 8:166–75.

Anderson, M. L. (2020). As the wind blows: The effects of long-term exposure to air pollution on mortality. *Journal of the European Economic Association*, 18:1886–1927.

Aragón, F. M., Miranda, J. J., and Oliva, P. (2017). Particulate matter and labor supply: the role of caregiving and non-linearities. *Journal of Environmental Economics and Management*, 86:295–309.

Arceo, E., Hanna, R., and Oliva, P. (2016). Does the effect of pollution on infant mortality differ between developing and developed countries? evidence from Mexico City. *The Economic Journal*, 126:257–280.

Baccini, M., Alessandra Mattei, F. M., Bertazzi, P. A., and Carugno, M. (2017). Assessing the short term impact of air pollution on mortality: a matching approach. *Environmental Health*, 16.

Banzhaf, S., Ma, L., and Timmins, C. (2019). Environmental justice: The economics of race, place, and pollution. *Journal of Economic Perspectives*, page 185–208.

Basaglia, P., Behr, S. M., and Drupp, M. A. (2025). Fuel taxation and environmental externalities: Evidence from the world's largest environmental tax reform. *CESifo Working Paper 11949*.

Bedi, A. S., Nakaguma, M. Y., Restrepo, B. J., and Rieger, M. (2021). Particle pollution and cognition: evidence from sensitive cognitive tests in brazil. *Journal of the Association of Environmental and Resource Economists*, 8:443–474.

Bell, M., Samet, J., and Dominici, F. (2004). Time-series studies of particulate matter. *Annual review of public health*, 25(1):247–80.

Brook, R. D., Rajagopalan, S., III, C. A. P., Brook, J. R., Bhatnagar, A., Diez-Roux, F. A. V., Holguin, F., Hong, Y., Luepker, R. V., Mittleman, M. A., Peters, A., Siscovick, D., Jr, S. C. S., Whitsel, L., and Kaufman, J. D. (2010). Particulate matter air pollution and cardiovascular disease: An update to the scientific statement from the american heart association. *Circulation*, 121:2331–2378.

Burkhardt, J., Bayham, J., Wilson, A., Carter, E., Berman, J. D., O'Dell, K., Ford, B., Fischer, E. V., and Pierce, J. R. (2019). The effect of pollution on crime: evidence from data on particulate matter and ozone. *Journal of Environmental Economics and Management*, 98:102267.

Calonico, S., Cattaneo, M. D., and Farrell, M. H. (2020). Optimal bandwidth choice for robust bias corrected inference in regression discontinuity designs. *The Econometrics Journal*, 23(2).

CARB (2021). Inhalable particulate matter and health (PM 2.5 and PM 10).

Cesaroni, G., Forastiere, F., Stafoggia, M., Andersen, Z. J., Badaloni, C., Beelen, R., Caracciolo, B., de Faire, U., Erbel, R., Eriksen, K. T., et al. (2014). Long term exposure to ambient air pollution and incidence of acute coronary events: Prospective cohort study and meta-analysis in 11 european cohorts from the escape project. *BMJ (Clinical research ed.)*, 348:f7412.

Chang, T., Zivin, J. G., Gross, T., and Neidell, M. (2016). Particulate pollution and the productivity of pear packers. *American Economic Journal: Economic Policy*, 8:141–169.

Chang, T. Y., Graff Zivin, J., Gross, T., and Neidell, M. (2019). The effect of pollution on

worker productivity: evidence from call center workers in China. *American Economic Journal: Applied Economics*, 11(1):151–172.

Chen, S., Oliva, P., and Zhang, P. (2022). The effect of air pollution on migration: Evidence from China. *Journal of Development Economics*, 156:102833.

Chen, S., Oliva, P., and Zhang, P. (2024). Air pollution and mental health: Evidence from china. *AEA Papers and Proceedings*, 114:423–428.

Crouse, D. L., Peters, P. A., Hystad, P., Brook, J. R., van Donkelaar, A., Martin, R. V., Villeneuve, P. J., Jerrett, M., Goldberg, M. S., III, C. A. P., Brauer, M., Brook, R. D., Robichaud, A., Menard, R., and Burnett, R. T. (2015). Ambient PM 2.5, O3, and NO2 exposures and associations with mortality over 16 years of follow-up in the Canadian Census Health and Environment Cohort (CanCHEC). *Environmental Health Perspectives*, 123.

Currie, J., Voorheis, J., and Walker, R. (2023). What caused racial disparities in particulate exposure to fall? new evidence from the clean air act and satellite-based measures of air quality. *American Economic Review*, 113(1):71–97.

de la Barrera, F., Barraza, F., Favier, P., Ruiz, V., and Quense, J. (2018). Megafires in chile 2017: Monitoring multiscale environmental impacts of burned ecosystems. *Science of The Total Environment*, 637–638:1526–1536.

Deryugina, T., Heutel, G., Miller, N. H., Molitor, D., and Reif, J. (2019). The mortality and medical costs of air pollution: Evidence from changes in wind direction. *American Economic Review*, 109(12):4178–4219.

Ebenstein, A., Lavy, V., and Roth, S. (2016). The long-run economic consequences of high-stakes examinations: evidence from transitory variation in pollution. *American Economic Journal: Applied Economics*, 8:36–65.

EPA (2009). Integrated science assessment for particulate matter. Technical report, United States Environmental Protection Agency. National Center for Environmental Assessment-RTP Division.

EPA (2010). Particle pollution and your health. Technical report, United States Environmental Protection Agency.

Graff Zivin, J. and Neidell, M. (2013). Environment, health, and human capital. *Journal of Economic Literature*, 51:689–730.

Gramsch, E., Cereceda-Balic, F., Oyola, P., and von Baer, D. (2006). Examination of pollution trends in santiago de chile with cluster analysis of pm10 and ozone data. *Atmospheric Environment*, 40:5464–5475.

Guidetti, B., Pereda, P., and Severnini, E. (2021). "placebo tests" for the impacts of air pollution on health: The challenge of limited health care infrastructure. *AEA Papers and Proceedings*, 111:371–375.

Hernandez-Cortes, D. and Meng, K. (2023). Do environmental markets cause environmental injustice? evidence from california's carbon market. *Journal of Public Economics*, 217:104786.

Herrnstadt, E., Heyes, A., Muehlegger, E., and Saberian, S. (2021). Air pollution and criminal activity: microgeographic evidence from chicago. *American Economic Journal: Applied Economics*, 13:70–100.

Hoffmann, B. and Rud, J. P. (2024). The unequal effects of pollution on labor supply. *Econometrica*, 92:1063–1096.

Kahn, M. E. and Li, P. (2020). Air pollution lowers high skill public sector worker productivity in China. *Environmental Research Letters*, 15(8):084003.

Lin, M., Chen, Y., Burnett, R. T., Villeneuve, P. J., and Krewski, D. (2002). The influence of ambient coarse particulate matter on asthma hospitalization in children: case-crossover and time-series analyses. *Environmental health perspectives*, 110(6):575–581.

Mazzeo, A., Huneeus, N., Orfanoz-Cheuquelaf, C. O., Menut, L., Mailler, S., Valari, M., van der Gon, H. D., Gallardo, L., Muñoz, R., Donoso, R., Galleguillos, M., Osses, M.,

and Tolvett, S. (2018). Impact of residential combustion and transport emissions on air pollution in santiago during winter. *Atmospheric Environment*, 190:195–208.

MMA (2015). Informe final para la gestión de episodios críticos de contaminación atmosférica por material particulado respirable (mp10). Technical report, Ministry of the Environment, Chile.

Mullins, J. and Bharadwaj, P. (2015). Effects of short term measures to curb air pollution: Evidence from santiago, chile. *American Journal of Agricultural Economics*, 97(4):1107–1134.

New York State Department of Health (2021). Fine particles (PM 2.5) questions and answers.

Pope, C. A. and Dockery, D. W. (2006). Health effects of fine particulate air pollution: Lines that connect. *Journal of the Air and Waste Management Association*, 56:709–742.

Riojas-Rodriguez, H., da Silva, A. S., Texcalac-Sangrador, J. L., and Moreno-Banda, G. L. (2016). Air pollution management and control in latin america and the caribbean: implications for climate change. *Rev Panam Salud Publica*, page 150–159.

Rivera, N. M. (2021). Air quality warnings and temporary driving bans: Evidence from air pollution, car trips, and mass-transit ridership in santiago. *Journal of Environmental Economics and Management*, 108.

Sager, L. (2019). Estimating the effect of air pollution on road safety using atmospheric temperature inversions. *Journal of Environmental Economics and Management*, 98:102250.

Sager, L. and Singer, G. (2025). Clean identification? the effects of the clean air act on air pollution, exposure disparities, and house prices. *American Economic Journal: Economic Policy*, 17(1):1–36.

Schwartz, J., Fong, K., and Zanobetti, A. (2018). A national multicity analysis of the causal effect of local pollution, no2 , andpm 2:5 on mortality. *Environmental Health Perspectives*, 126:077011.

Sharma, S., Chandra, M., and Kota, S. H. (2020). Health effects associated with pm2.5: a systematic review. *Current Pollution Reports*, 6:345–367.

Southerland, V. A., Brauer, M., Mohegh, A., Hammer, M. S., van Donkelaar, A., Martin, R. V., Apte, J. S., and Anenberg, S. C. (2022). Global urban temporal trends in fine particulate matter (pm2·5) and attributable health burdens: estimates from global datasets. *Lancet Planet Health*, 6:e139–46.

Tertre, A. L., Medina, S., Samoli, E., Forsberg, B., Michelozzi, P., Boumghar, A., Vonk, J., Bellini, A., Atkinson, R., Ayres, J., Sunyer, J., Schwartz, J., and Katsouyanni, K. (2002). Short-term effects of particulate air pollution on cardiovascular diseases in eight European cities. *Journal of epidemiology and community health*, 56:773–9.

Toro, R., Kvakić, M., Klaić, Z. B., Koračin, D., S, R. G. E. M., and G, M. A. L. (2019). Exploring atmospheric stagnation during a severe particulate matter air pollution episode over complex terrain in santiago, chile. *Environmental Pollution*, 244:705–714.

Tracy, T. and Layton, D. W. (1995). Deposition, resuspension, and penetration of particles within a residence. *Atmospheric Environment*, 29(13):1487–1497.

Trujillo, J. L., Parilla, J., and Razmilic, S. (2016). Global santiago profiling the metropolitan region's internationa competitiveness and connections. Technical report, Brookings Institution and JP Morgan Chase.

Vette, A., Rea, A., Lawless, P., Rodes, C., Evans, G., Highsmith, V., and Sheldon, L. (2001). Characterization of indoor-outdoor aerosol concentration relationships during the Fresno PM exposure studies. *Aerosol Science and Technology*, 34:118–126.

Wei, Y., Wang, Y., Xiao Wu, Q. D., Shi, L., Koutrakis, P., Zanobetti, A., Dominici, F., and Schwartz, J. D. (2020). Causal effects of air pollution on mortality rate in massachusetts. *American Journal of Epidemiology*, 189:1316–1323.

WHO (2021). Who global air quality guidelines. particulate matter (pm 2.5 and pm 10), ozone, nitrogen dioxide, sulfur dioxide and carbon monoxide. World Health Organization.

Yuan, L., Zhang, Y., Gao, Y., and Tian, Y. (2019). Maternal fine particulate matter (pm2.5) exposure and adverse birth outcomes: an updated systematic review based on cohort studies. *Environmental science and pollution research international*, pages 13963–13983.

Zhang, X., Zhang, X., and Chen, X. (2017). Happiness in the air: How does a dirty sky affect mental health and subjective well-being? *Journal of Environmental Economics and Management*, 85:81–94.

Zivin, J. G., Liu, T., Song, Y., Tang, Q., and Zhang, P. (2020). The unintended impacts of agricultural fires: Human capital in China. *Journal of Development Economics*, 147:102560.

A Tables

Table A.1: Share of Individuals Working Nearest to Each Station, by Income Decile

Income decile	CER	CEN	BOS	IND	FLO	CON	PAO	PUD	PUA	QUI	TAL	Count
D1	13.7	5.5	14.9	16.1	16.6	3.6	12.6	6.1	6.4	2.4	2.0	1894
D2	2.6	5.8	10.3	20.4	7.3	2.0	16.0	5.0	19.0	8.2	3.3	1894
D3	9.6	8.0	12.1	20.2	10.4	2.0	15.8	6.4	9.3	3.7	2.5	1894
D4	7.7	5.5	11.8	20.3	11.9	4.9	15.0	4.9	12.8	3.6	1.5	1894
D5	6.3	3.5	11.0	26.2	11.2	7.5	17.3	3.1	6.6	5.5	1.7	1894
D6	7.0	4.4	9.3	27.1	10.6	7.9	16.5	4.1	6.3	5.2	1.6	1894
D7	7.0	3.9	7.0	27.4	10.9	8.1	18.2	3.8	7.0	5.1	1.7	1894
D8	5.4	3.5	6.2	31.5	8.7	8.2	16.3	3.3	7.8	8.0	1.1	1894
D9	4.7	2.7	6.3	35.1	9.5	8.9	15.5	4.1	6.4	6.1	0.7	1894
D10	3.0	2.1	4.2	40.2	8.1	14.5	16.8	2.1	4.4	4.1	0.6	1894

Notes: This table reports the share of individuals whose "work" locations is nearest to each monitor by income decile. Income deciles are computed from the EOD microdata using individual per-capita income (total household income divided by the number of household members). The sample includes only adults aged 25+ whose residence and every reported location on the reference day are within 5 km of at least one monitoring station. The counts in the last column are the exact number of individuals in each decile.Residential coordinates are inferred as described in Section 4.1. The "work location" is assigned from the itinerary on the reference day: we select the most frequent location across the 24-hour day. If this coincides with the home location, we use the second-most frequent location. Within each decile, station shares sum to 100%.

Table A.2: Share of Individuals Living Nearest to Each Station, by Income Decile

Income decile	CER	CEN	BOS	IND	FLO	CON	PAO	PUD	PUA	QUI	TAL	Count
D1	16.6	6.4	17.5	9.5	20.4	4.0	3.3	8.4	7.9	3.7	2.2	1894
D2	2.3	9.5	12.1	11.7	6.1	1.7	9.7	7.4	24.9	10.9	3.8	1894
D3	11.7	11.2	14.6	12.0	11.7	0.9	7.9	9.0	13.3	5.1	2.6	1894
D4	10.9	8.8	16.1	8.1	12.2	1.3	6.7	8.2	22.0	4.1	1.7	1894
D5	6.8	6.7	20.6	11.8	13.3	1.7	8.0	5.6	16.2	6.7	2.6	1894
D6	11.2	8.0	14.8	11.2	14.6	3.0	7.3	6.5	16.2	5.2	2.0	1894
D7	10.9	7.4	10.8	13.7	13.8	1.8	8.3	8.2	16.6	6.0	2.4	1894
D8	7.8	5.4	10.2	14.1	16.7	3.9	8.6	6.4	15.8	9.5	1.6	1894
D9	6.8	5.3	7.3	17.4	17.5	6.6	11.6	5.5	13.6	7.4	0.9	1894
D10	3.5	2.2	4.7	24.4	14.8	21.2	13.0	3.0	8.7	4.2	0.3	1894

Notes: This table reports the shares of individuals whose "residence location" is nearest to each monitor by income decile. Income deciles are computed from the EOD microdata using individual per-capita income (total household income divided by the number of household members). The sample includes only adults aged 25+ whose residence and every reported location on the reference day are within 5 km of at least one monitoring station. The counts in the last column shows the exact number of individuals in each decile.Residential coordinates are either observed or inferred from "return home" trips; if a respondent does not report one, we use a household member's "return home" trip, and if none exists, the first reported origin is considered the residential location (see Section 4.1). Roughly 75% of adults 25+ have an observed or inferred residence. Within each decile, station shares sum to 100%.

Table A.3: First Stage Results – Daily Data - All Calendar Months

	(1)	(2)
	Probability of an episode in day t	
Second stage outcome	*PM_{10} mean*	*$PM_{2.5}$ mean*
$ICAP10_{t-1} \geq 0$	0.242	0.306**
	(0.182)	(0.148)
Observations	117	145
Weather controls	✓	✓
F statistic	13	16
Bandwidth	Optimal = 45.69	Optimal = 55.06

Notes: This table reports the first stage results for our fuzzy regression discontinuity design using daily data for all months. The running variable is the daily maximum $ICAP_{10_{t-1}}$. The first stage dependent variable is a dummy for whether there was an episode with restrictions in place on day t. The second stage outcome differs across columns. The second stage outcome is the daily mean PM_{10} in column (1) and is the daily mean $PM_{2.5}$ for column (2). Each column uses a different bandwidth around the cutoff ($c = 0$). Columns (1) and (2) uses the optimal bandwidth following Calonico et al. (2020). Robust standard errors in parentheses. * $p < 0.1$, ** $p < 0.05$, *** $p < 0.01$.

Table A.4: City-Wide Second Stage Results: Daily Data - All Calendar Months

	PM_{10}			$PM_{2.5}$		
	Mean	Max	Mean 8am-8pm	Mean	Max	Mean 8am-8pm
$\hat{P}(\text{episode}_t)$	-0.093**	-0.065	-0.035	0.020	-0.039	0.013
	(0.034)	(0.044)	(0.041)	(0.042)	(0.058)	(0.047)
Observations	117	111	117	145	141	145
Weather controls	✓	✓	✓	✓	✓	✓
Outcome mean	4.12	5.32	4.18	3.18	4.32	3.14
Optimal bwd	45.69	42.48	45.71	55.06	54.06	55.21

Notes: This table reports the city-wide second stage results for our fuzzy regression discontinuity design using daily data for all months. See Section 5.1.1 for a detail description of the city-wide specification. All columns report the results using the optimal bandwidth for each outcome.

Table A.5: Daily Effect of a Critical Episode on PM_{10} and $PM_{2.5}$, by Station - All Calendar Months

	QUI		PUD		CEN		CER		IND		PAO		BOS		FLO		PUA		CON	
	PM10	PM2.5	PM10	PM2.5	PM10	PM2.5	PM10	PM2.5	PM10	PM2.5	PM10	PM2.5	PM10	PM2.5	PM10	PM2.5	PM10	PM2.5	PM10	PM2.5
$P(\widehat{episode}_t)$	0.077*	-0.002	-0.080	-0.051	-0.051	-0.037	0.067*	0.091	-0.056*	-0.078**	-0.061	-0.004	0.047	0.103*	-0.012	-0.084	-0.108**	-0.019	-0.131**	-0.253***
	(0.040)	(0.053)	(0.050)	(0.051)	(0.037)	(0.032)	(0.034)	(0.057)	(0.030)	((0.035))	(0.043)	(0.036)	(0.034)	(0.060)	(0.034)	(0.058)	(0.045)	(0.060)	(0.046)	(0.053)
Elevation	491	491	491	491	500	500	513	513	553	553	558	558	580	580	606	606	672	672	799	799
Mean education level (census geographic area)	10.489	10.489	10.186	10.186	10.019	10.019	10.744	10.744	12.003	12.003	9.789	9.789	10.993	10.993	12.375	12.375	12.616	12.616	15.391	15.391
Observations	108	132	80	95	96	121	101	125	104	125	105	124	106	129	97	99	92	116	95	119
Outcome mean	4.287	3.145	4.065	3.127	4.047	3.176	4.114	3.208	4.058	3.159	4.164	3.177	4.192	3.255	4.171	3.199	4.055	3.194	3.878	2.999
Optimal bandwidth	45.69	55.06	45.69	55.06	45.69	55.06	45.69	55.06	45.69	55.06	45.69	55.06	45.69	55.06	45.69	55.06	45.69	55.06	45.69	55.06

Notes: This table reports the second stage results at the station-level following the empirical strategy described in Section 5.1.2 using daily data for all months. All columns report the results using the optimal bandwidth at each side of the cutoff (c=0). This optimal bandwidth is the same for all stations and comes from the optimal bandwidth at the city-wide daily level.

B Figures

Figure B.1: Critical Air Quality Episodes and Daily Maximum ICAP PM10, 2009–2014

(a) 2009

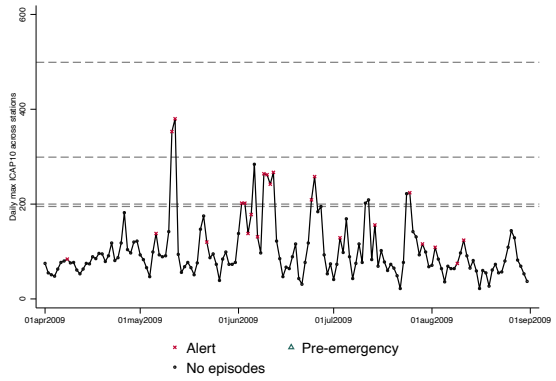

(b) 2010

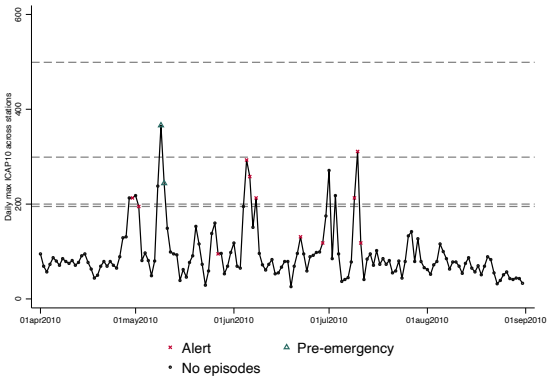

(c) 2011

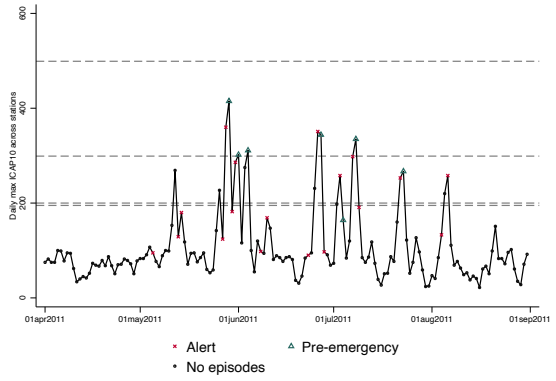

(d) 2012

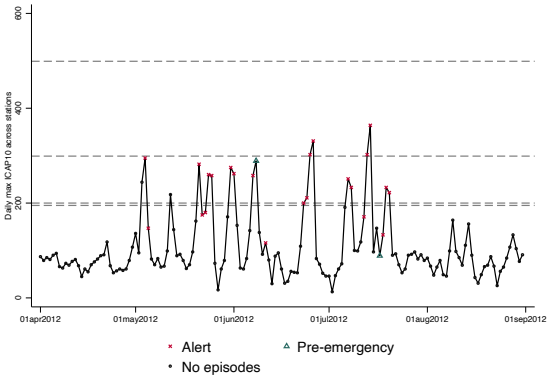

(e) 2013

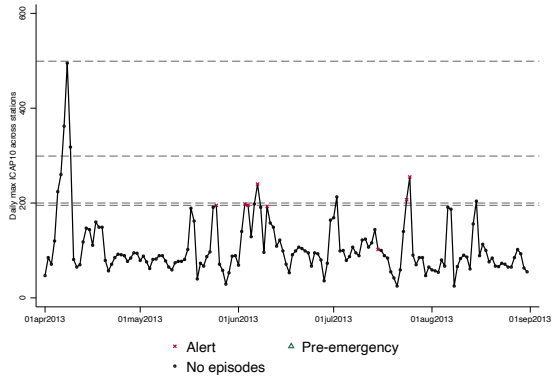

(f) 2014

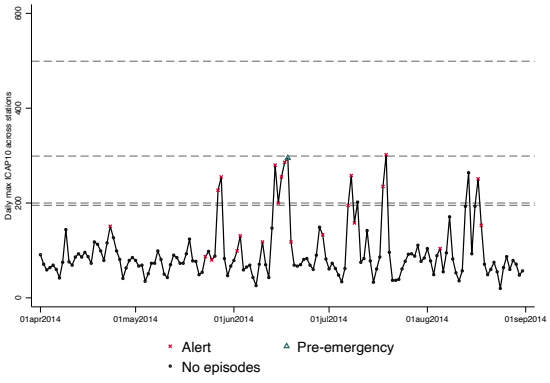

Notes: Each figure plots the daily maximum PM_{10} ICAP level in day t and the days with restrictions (i.e. episodes) on day t during winter periods of 2009-2015. The daily maximum PM_{10} ICAP was built following the MMA criteria described in Section 3.1.

Source: Data on PM10 levels were collected from SINCA and data on air quality episodes from MMA.

Figure B.2: Mean Exposure to PM2.5 and PM10 in 2012 Using a 20 km Radius, by Income Deciles

(a) PM2.5 Mean

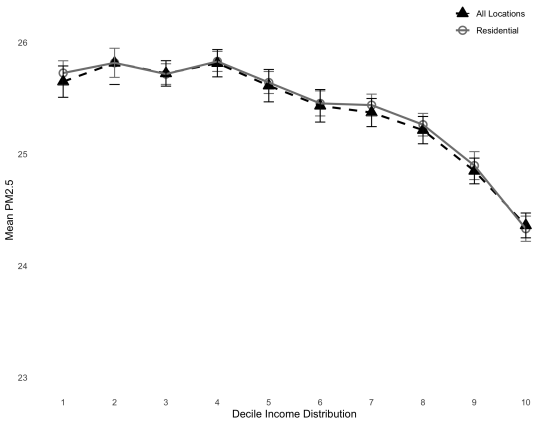

(b) PM10 Mean

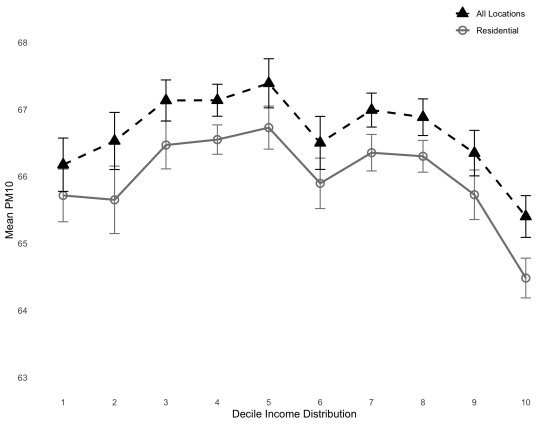

Source: Encuesta Origen - Destino a Hogares (EODH), 2012; pollution data from SINCA, 2012.

Notes: This figure plots annual mean exposure to PM2.5 and PM10 across income deciles using a 20 km radius around monitoring stations. "Residential" refers to the exposure measured at an individual's residence as reported in the survey. "All locations" represents the individual's actual location during the reference day as reported in the EOD survey. Exposure values are computed using inverse quadratic distance weighting from all monitoring stations within the specified radius. Individuals are included in the sample if all of their locations reported during the reference day are within 20 km of a monitoring station and they are at least 25 years old. Sampling survey weights are applied.

Figure B.3: Hourly Mean Pollution Levels by Station

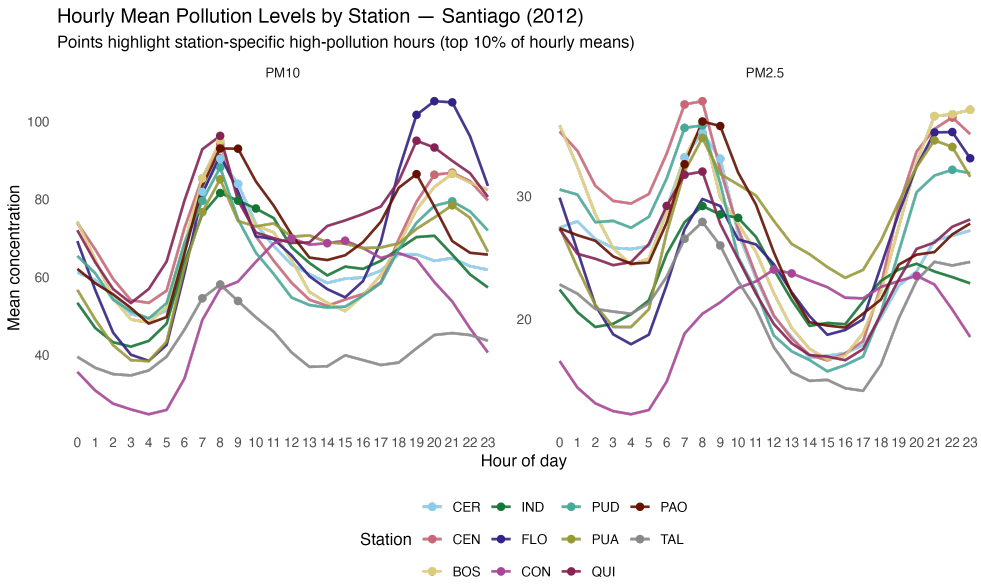

Notes: Each panel reports hourly means for PM_{10} (left) and $PM_{2.5}$ (right) for each station in 2012. Dots mark station-specific high-pollution hours (top 10% of hourly means). The x-axis is hour of day (0–23); y-axes are in $\mu g/m^3$.

Figure B.4: Hourly Effect of an Air Quality Critical Episode on PM_{10}, by Station - All Calendar Months

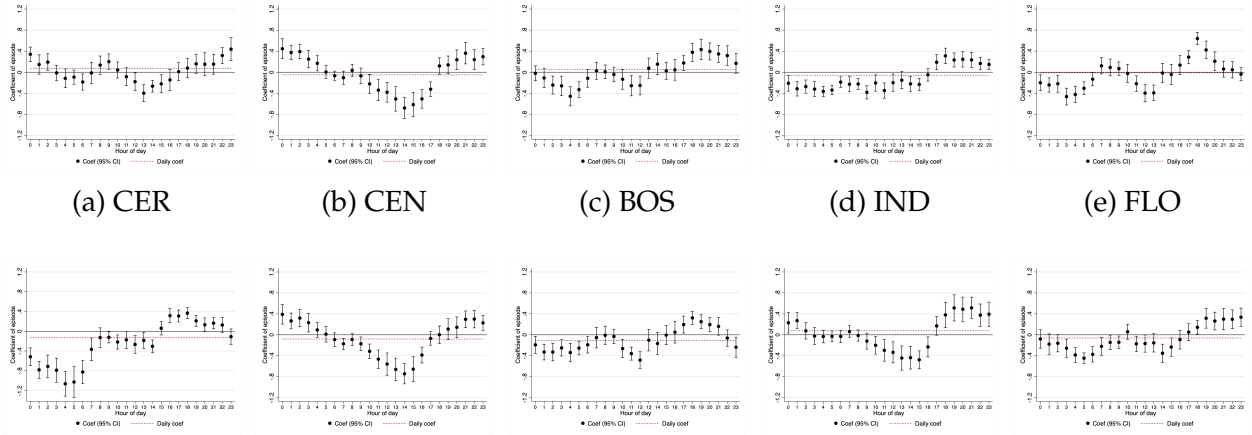

(a) CER (b) CEN (c) BOS (d) IND (e) FLO

(f) CON (g) PUD (h) PUA (i) QUI (j) PAO

Notes: Each panel plots the PM_{10} second-stage results for a monitoring station following the empirical strategy described in Section 5.1.2 using hourly data for all months. All columns report the results using the optimal bandwidth on each side of the cutoff ($c = 0$). This optimal bandwidth is the same for all stations and is based on the optimal bandwidth estimated at the citywide daily level.

Figure B.5: Hourly Effect of an Air Quality Critical Episode on $PM_{2.5}$, by Station - All Calendar Months

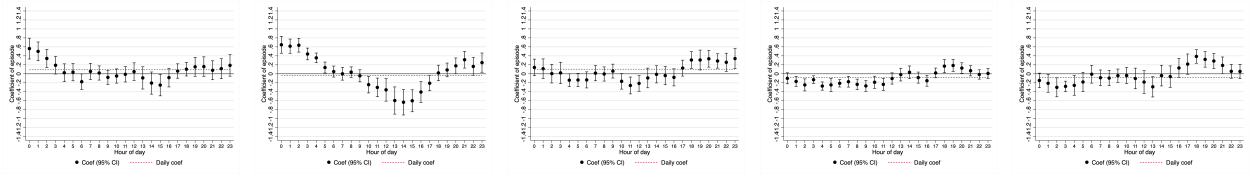

(a) CER (b) CEN (c) BOS (d) IND (e) FLO

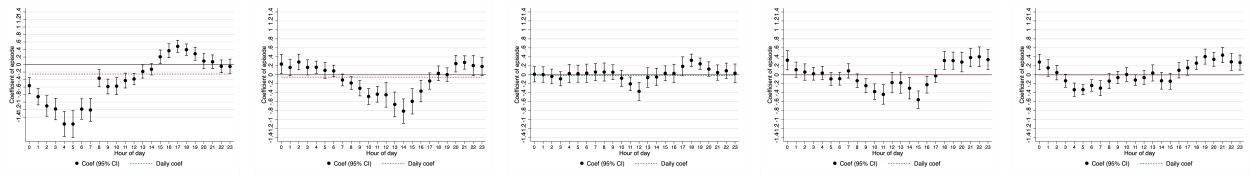

(f) CON (g) PUD (h) PUA (i) QUI (j) PAO

Notes: Each panel plots the second-stage results for $PM_{2.5}$ at the station level for each station, following the empirical strategy described in Section 5.1.2, using hourly data for all months. All columns report the results using the optimal bandwidth on each side of the cutoff ($c = 0$). This optimal bandwidth is the same for all stations and is based on the optimal bandwidth estimated at the citywide daily level.

Figure B.6: Hourly Effect of an Air Quality Critical Episode on $PM_{2.5}$ for Representative Individuals of Each Income Decile

(a) Decile 1 (b) Decile 2 (c) Decile 3 (d) Decile 4 (e) Decile 5

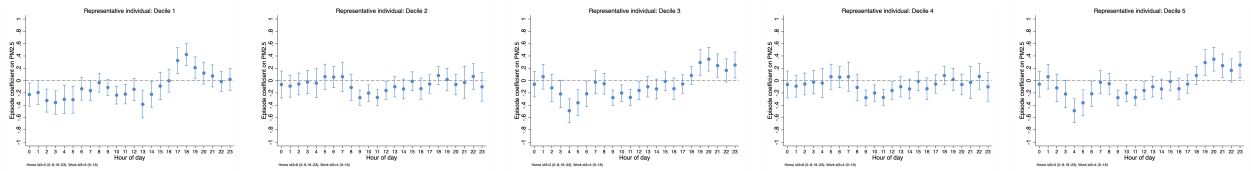

(f) Decile 6 (g) Decile 7 (h) Decile 8 (i) Decile 9 (j) Decile 10

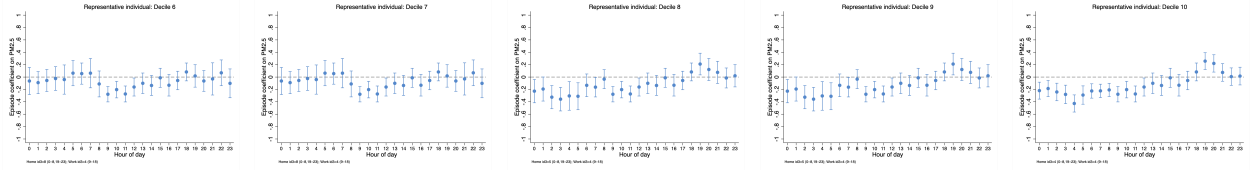

Notes: Each panel plots the $PM_{2.5}$ second-stage results for the representative individual of an income deciles following the empirical strategy described in Section 5.1.2 and using hourly data for the winter months. All columns report the results using the optimal bandwidth on each side of the cutoff ($c = 0$). This optimal bandwidth is the same for all stations and is based on the optimal bandwidth estimated at the citywide daily level.

C Data Appendix

3.1 Air Quality from the Metropolitan Area of Gran Santiago

Air quality data for Santiago is obtained from the *Sistema de Información Nacional de Calidad del Aire* (SINCA), maintained by the *Ministerio del Medio Ambiente* (MMA) of Chile. The data is available through the SINCA platform at `https://sinca.mma.gob.cl/index.php/region/index/id/M`. We accessed the air quality data in January 2020.
To replicate the pollution datase:

1. Use the region-specific menu to filter monitoring stations in the Metropolitan Region.
2. Select pollutants PM_{10} and $PM_{2.5}$, along with our sample period (2009-2015).
3. Download the hourly data for each pollutant and station.

3.2 Spatial Aggregation of Air Quality Data

We assign hourly $PM_{2.5}$ and PM_{10} exposure to individuals in the 2012 *Encuesta de Origen–Destino* (EOD) using missingness–aware inverse–distance–squared weighting (IDW). We begin by describing the steps that we follow, and we include the mathematical details below.

Operational steps.

1. **Identify monitoring stations.** All stations in the 2012 network reported PM2.5 and PM10 data during the year and are eligible a priori.
2. **Proximity filter (baseline and robustness).** Keep individuals whose residential coordinates and all location coordinates lie within a given radius of *at least one* monitor. We use a $R = 5\,\text{km}$ radius for our main results and we use a $R = 20\,\text{km}$ radius for robustness.

3. **Weights.** For each location in our data, we determine the great–circle distance d from that location to each station. Only stations within R receive positive weight. For each station within R, the station's weight is $w = 1/\max(d, \varepsilon)^2$, with a small floor ε (e.g., 20–30 m) to avoid dividing by zero in any case any individual reports a location exactly the same as a monitoring station.

4. **Hourly exposure.** For each location-hour in our data, we compute a *normalized* IDW average using only the stations that report PM2.5 (or PM10) in that hour. A station that has missing data for that pollutant at hour t receives zero effective weight at t.

5. **Annual summary statistics.** The annual *mean* is the exact time–average of the hourly series over 2012 (see the weighted formula below). "Median" summaries are defined consistently with the analysis grouping: *per–day* median (across that day's 24 hours), *per–hour–of–day* median (across days for a fixed clock hour), or an *all–year* median (across every hour of 2012).

3.2.1 Mathematical formulation (concise)

Let $x_{t,j}$ be the pollutant reading at station j in hour t. For individual i, let $d_{i,j}^{(t)}$ be the distance from i's location at hour t to station j (the "All–Locations" hypothesis). Define inverse–square weights

$$w_{i,j}^{(t)} := \frac{1}{\max\left(d_{i,j}^{(t)}, \varepsilon\right)^2},$$

with small $\varepsilon > 0$, and let $\mathbb{1}[\cdot]$ indicate that a station's hourly reading is observed (non–missing).

Residential hypothesis (special case). If individuals are assumed to remain at home, then distances do not vary over time: $d_{i,j}^{(t)} \equiv d_{i,j}$ and $w_{i,j}^{(t)} \equiv w_{i,j}$.

Hourly exposure (missingness–aware normalized IDW)

All Locations (time–varying distances):

$$E_{i,t}^{\text{all}} \;=\; \frac{\sum_j w_{i,j}^{(t)}\, x_{t,j}\, \mathbb{1}[x_{t,j} \text{ observed}]}{\sum_j w_{i,j}^{(t)}\, \mathbb{1}[x_{t,j} \text{ observed}]}\,. \tag{9}$$

Residential (time–invariant distances):

$$E_{i,t}^{\text{res}} \;=\; \frac{\sum_j w_{i,j}\, x_{t,j}\, \mathbb{1}[x_{t,j} \text{ observed}]}{\sum_j w_{i,j}\, \mathbb{1}[x_{t,j} \text{ observed}]}\,. \tag{10}$$

Both expressions are normalized weighted averages: they preserve units, automatically re-weight to the set of stations that report at hour t, and return c whenever all available stations read the common value c.

Time aggregation: means and medians

Annual mean (coverage–consistent). Let $D_{i,t} = \sum_j w_{i,j}^{(t)} \mathbb{1}[x_{t,j} \text{ observed}]$ denote the effective weight mass in hour t. The exact annual mean is the *coverage–weighted average* of hourly exposures:

$$\overline{E}_i^{\text{mean}} \;=\; \frac{\sum_t E_{i,t}\, D_{i,t}}{\sum_t D_{i,t}} \;=\; \frac{\sum_t \sum_j w_{i,j}^{(t)}\, x_{t,j}\, \mathbb{1}[x_{t,j} \text{ observed}]}{\sum_t \sum_j w_{i,j}^{(t)}\, \mathbb{1}[x_{t,j} \text{ observed}]}\,.$$

Intuition: hours with more (closer) reporting stations receive more weight; hours with little or no coverage receive little or none.